Optical Multiplexing Anti-Counterfeiting Film Based on Self-Assembled and Holography Lithographic Photonic Architectures

Xiaowan Xu, Yanjun Liu, *Senior Member, IEEE*, and Dan Luo

***Abstract*—Multiplexing anti-counterfeiting technologies based on micro/nano structural colors of photonic crystals have been proposed for information security because of unduplicability and diversity. However, most of current fabrication methods for micro/nano structural color such as electronic beam etching and ordered nanoparticles are accompanied with expensive and complex fabrication process. Reliable multiplexing anti-counterfeiting technologies with low cost and easy-fabrication process for currency, brands and information security remain a long-time and innovative challenge. Herein, a simple strategy to fabricate optical multiplexing anti-counterfeiting film based on self-assembled three-dimensional photonic crystal BPLC encoded with holography lithographic 1D/2D surface photonic crystal has been proposed. The proposed bilayer structure can exhibit multi-images with different angles in 3D space, leading to multiple encryptions with information protection or access permission. Quick response (QR) code with cryptographic functionality through our proposed multiplexing anti-counterfeiting film based on bilayer structural color is also demonstrated. The proposed strategy for optical multiplexing anti-counterfeiting film is low-cost, easy-fabricated, time saving, stable and flexible, capable for promising perspective in information security level and storage density, and offering potential application in anti-counterfeiting.**

***Index Terms*—Liquid crystals, polymers, photonic crystals.**

I. Introduction

A LARGE amount of counterfeiting products spread over our daily life, which seriously influences the property safety, society stability, and even threatens human health. It is reported that the global economic losses caused by counterfeiting would reach to 1.82 trillion dollars in 2020 [1], [2]. Traditional anti-counterfeiting strategies, such as watermarks, barcodes, two-dimensional codes, and hologram labels, are easily to be copied [3]–[5]. Therefore, developing reliable anti-counterfeiting is highly demanded. Among plenty of technologies, optical multiplexing anti-counterfeiting technology, which processes multiple images delivering from a single material, provides the spatial distribution of light information via different channels for store and deliver data. It leads to higher difficulties of decryption and provides a new solution for information security level or storage density and offers potential applications.

The common optical multiplexing anti-counterfeiting products are usually based on several strategies such as luminescent materials [6], [7], micro/nano structures [8], [9], and meta materials [10]. For example, Lang Qin and the coworkers [11] proposed a two-tone geminate label based on the structural color of chiral nematic liquid crystal microdroplets and fluorescent materials. This label had two different images under natural light and ultraviolet light which ensured the information security. Xintao Lai and his coworkers [12] fabricated two dimensional self-assemble nano-sized spheres and nanoimprinted micro-structures into quasi-3D multiplexing anti-counterfeiting imaging. This anti-counterfeiting product has different images with 0° and 90° polarization. Among these anti-counterfeiting strategies, structural colors of micro/nano structures have attracted much attention because of easily recognition by visual perception of human eyes, which have long-term stability, environmentally friendly properties and high optical qualities compared to luminescent materials [13]–[15], and meta materials [16], [17].

However, traditional fabrication methods for structural color based on micro/nano structure, like mechanical drilling [18], are hard to realize nanostructures for visible light range. Precise nano-fabrications, like electron beam etching [19], need expensive instrument and high time cost which is against commercial use. Though self-assemble colloidal nanoparticles into ordered colloidal photonic crystal (PC) structures are cost-save methods, they need additional self-assemble fabrications, such as sedimentation [20], inkjet printing [21], and air-water interface method [22] and so on, which always rely on the substrate and are easy to generate defects. Therefore, simple and low-cost nano-fabrication method for structural color-based optical multiplexing anti-counterfeiting product remains a challenge.

Blue phase liquid crystals (BPLCs) are self-assembled three-dimensional (3D) photonic crystals with intrinsic property of simple fabrication process and low cost, which is capable of exhibiting structural colors from ultraviolet (UV) light to visible light. The BPLC simply emerges between isotropic phase and cholesteric phase of chiral nematic liquid crystal, which

Manuscript received March 28, 2022; revised April 15, 2022; accepted April 22, 2022. Date of publication April 26, 2022; date of current version May 5, 2022. This work was supported in part by the National Natural Science Foundation of China under Grant 61875081, and in part by Guangdong Basic and Applied Basic Research Foundation under Grant 2021B1515020097. *(Corresponding author: Dan Luo.)*

Xiaowan Xu is with the Electronic Science and Technology, Harbin Institute of Technology, Harbin, Heilongjiang 518071, China, and also with the Department of Electrical & Electronic Engineering, Southern University of Science and Technology, Shenzhen, Guangdong 518055, China (e-mail: xuxiaowan_1@163.com).

Yanjun Liu and Dan Luo are with the Department of Electrical & Electronic Engineering, Southern University of Science and Technology, Shenzhen, Guangdong 518055, China (e-mail: yjliu@sustech.edu.cn; luod@sustech.edu.cn).

Digital Object Identifier 10.1109/JPHOT.2022.3170269

assembles blue phase I (BPI) and blue phase II (BPII) with body-centered and simple cubic crystal, exhibits uniform 3D PC structures [23], [24]. Usually, the polymer is applied to broaden the narrow temperature range of BPLC to larger than 60 °C (including room temperature), or called polymer-stabilized BPLC (PS-BPLC), which enables structural color devices with properties of stretchability [25]–[27], tenability [28]–[30], and compressibility [31]–[33]. Therefore, the self-assembled 3D PC BPLC film becomes a potential candidate for fabrication of optical multiplexing anti-counterfeiting product due to simple fabrication process, low cost, and uniformity.

In this paper, a simple strategy to fabricate optical multiplexing anti-counterfeiting film based on self-assembled three-dimensional photonic crystal BPLC encoded with holography lithographic 1D/2D surface photonic crystal has been proposed. 1D/2D surface photonic crystal with different shape can be easily encoded by holography lithographic technology on the surface of 3D self-assembled photonic crystal BPLC to form a bilayer structure with multi-structural colors. The proposed bilayer structure can exhibit multi-images with different angles in 3D space, leading to multiple encryptions with information protection or access permission. Quick response (QR) code with cryptographic functionality through our proposed multiplexing anti-counterfeiting film based on bilayer structural color is also demonstrated. The proposed strategy for optical multiplexing anti-counterfeiting film is low-cost, easy-fabricated, time saving, stable and flexible, capable for promising perspective in information security level and storage density, and offering potential application in anti-counterfeiting.

II. Experiment

In the experiment, a BPLC film (with thickness of 5 μm) in BPI with body-centered cubic crystal structure (3D PC) is fabricated via wash out-refill method as the substrate film, as shown in Fig. 1(a). Firstly (step i), the liquid crystal mixture M1 (seeing materials section) is instilled in a liquid crystal cell consisted of two glass substrates with the thickness of 5 μm. The cell is heated over the clearing point of M1 (80 °C), and cooled down 0.1 °C per minute until uniform BPI is full of the cell. Then the sample is exposed under UV light (365 nm, 1 mW, 15 minutes) for polymerization. After polymerization, the cell is immersed in toluene to wash out the unpolymerized materials. The left material in the cell is polymer scaffold with BPI structure. In step ii, the liquid crystal mixture M2 is instilled in the scaffold BPI structure, and the cell is exposed under UV light to be polymerized again. After opening the cell by removing a glass substrate, an all solid and flexible BPLC film (3D PC) with high-reflectance (about 45%) and a large temperature range ($-50\sim260$ °C) is obtained. It is noticed that, the reflectance of the BPLC film is no more than 50% theoretically due to chiral property of BPLC that will only reflect the light with the same circularly polarization [34], [35].

Then, the 1D/2D PC structures are fabricated on the surface of the BPLC film by holographic lithography, as shown in Fig. 1(b). The 3D PC BPLC film on one substrate is treated under O_2 plasma for 30s to improve the affinity of photoresist, and spin coated with photoresist with thickness of 300 nm. The 1D/2D surface PC will be encoded on the 3D PC BPLC film through holographic lithography. The fabrication process of 1D surface PC is shown in step i: two-beam interference (by 325 nm UV laser) is applied on the photoresist to form 1D PCs (grating),

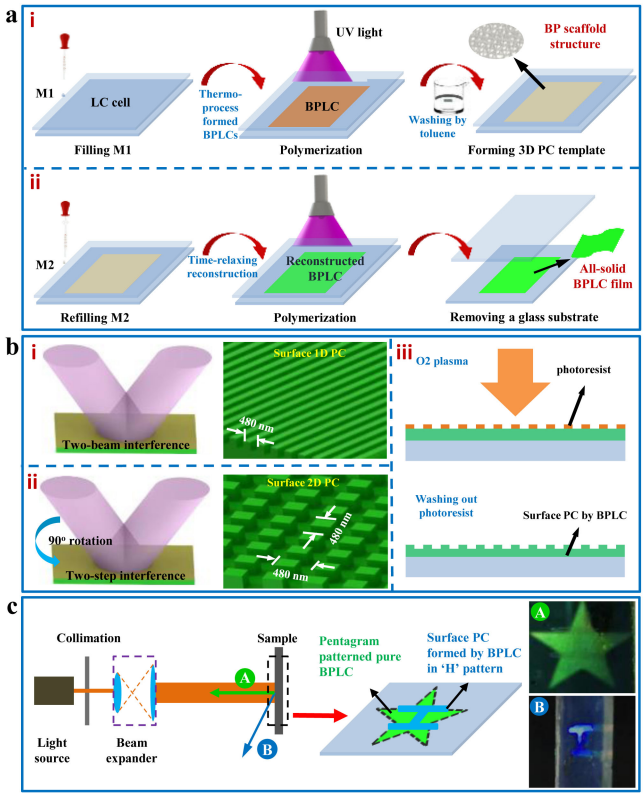

Fig. 1. (a) Fabrication of BPLC film. Step i: Firstly, fill liquid crystal mixture M1 into the LC cell; and polymerize the BPLC sample by UV light at the temperature of blue phase; then immerse the sample in toluene to remove unpolymerized materials; at last, the 3D PC template with BP scaffold structure is achieved. Step ii: Firstly, refill liquid crystal mixture M2 into the cell; and polymerize the BPLC sample by UV light again; then remove glass substrate; at last, the 3D PC film is obtained. (b) Fabrication of surface PCs: Step i: two-beam interference for 1D PC fabrication. Step ii: two-step interference for 2D PC fabrication by rotating the sample of 90° (inserted figures are schematic illustration of surface 1D and 2D PC, respectively). Step iii: the photoresist is etched by O_2 plasma, and after washing out the residual photoresist, the photonic structure combined with 3D PC BPLC and surface 1D/2D surface PCs is obtained. (c) Schematic illustration of the multiplexing anti-counterfeiting film consisted of photonic structure combined with 3D PC BPLC (in pentagram pattern) and 1D surface PCs ("H" pattern) in illumination of a white LED light with normal incidence. Inserted figure A: the pentagram patterned image of 3D PC BPLC in green color when observing from normal direction. Inserted figure B: the "H" image of 1D surface PC in blue color when observing from 60° with the normal direction).

and the angle between two beams is decided according to the equation of interference: $2d\sin\theta = \lambda$, where d is the period of grating, θ is the interference angle and λ is the wavelength of incident light. In addition, the fabrication process of 2D surface PC is shown in step ii: the 2D surface PC can be fabricated by two-step lithography with additional two-beam interference by rotating the substrate of 90° based on the 1D PC grating. The general fabrication process of surface PC is summarized in step iii: The O_2 plasma was used to etch the patterns of surface PCs on photoresist. At last, the residual photoresist is washed out, resulting in a 3D PC BPLC film encoded with the pattern of surface 1D/2D PC. In our experiment, θ is 19.8°, λ is 325 nm, leading to a calculated d of 480 nm, with duty ratio about 1:1. Each channel of 1D PC is about 240 nm and square of 2D PC is 240 nm $\times$ 240 nm (with lattice constant of 480 nm) which are approximately equal to the lattice size of the BPLC PCs.

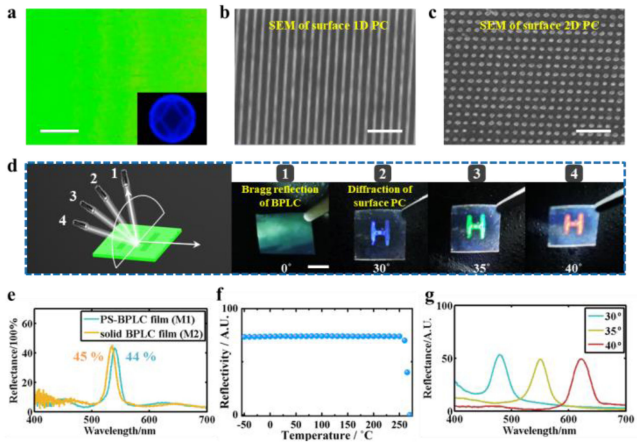

Fig. 2. (a) POM image of the BPLC film; inserted figure is Kossel diagram of BPI [011] orientation, scale bar: 200 μm. (b) SEM image of surface 1D PC, scale bar is 2 μm; (c) SEM image of surface 2D PC, scale bar is 2 μm. (d) The schematic situation and photos of the combined structures with multi-angles; inserted figures: BPLC film with surface 1D PCs in character of "H" depicting (1) Bragg reflection of BPLC (0°); (2) diffraction of surface 1D PCs (30°), (3) 35°, and (4) 40°, scale bar: 5 mm. (e) Reflective spectra of PS- and solid BPLC film. (f) The reflectivity at peak wavelength of solid BPLC film versus temperature from −50 °C to 260 °C. (g) Reflectance spectra from the surface 1D PC with diffractive angles of 30°, 35°, and 40°.

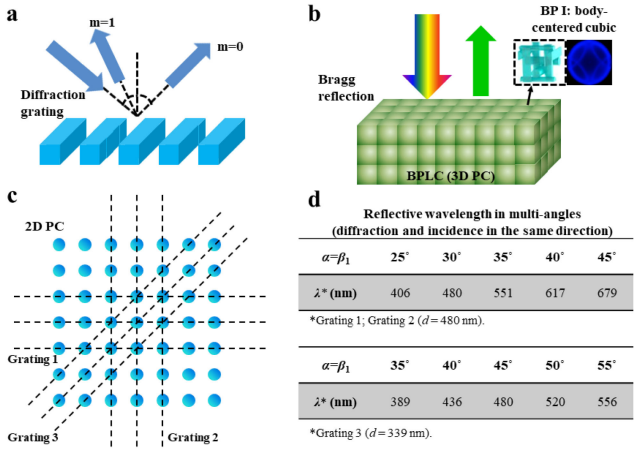

Fig. 3. (a) Reflection of surface 1D PC (diffractive grating). (b) Bragg reflection of 3D PC BPLC. The inset figures are body-centered cubic structure and Kossel diagram of BPI. (c) Schematic illustration of surface 2D PC (combined gratings in three directions). (d) Reflective wavelength of surface PCs in multi-angles when diffraction and incidence are in the same direction.

Fig. 1(c) depicts the schematic illustration of the multiplexing anti-counterfeiting film consisted of photonic structure combined with 3D PC BPLC (in pentagram pattern) and 1D surface PCs ("H" pattern) in illumination of a white LED light with normal incidence. The incident light is provided by a white LED light source after collimation of aperture and beam expander. When the white light incidents along the normal direction, two different images or multiplexing images can be observed from the normal direction (top view) or with certain angle of the normal direction (side view). The image observed from the normal direction is shown in inset figure A as the pentagram patterned image of 3D PC BPLC in green color, which is due to the selectively reflected from pure 3D PC BPLC. On other side, the image observed from the side view (60° with the normal direction) is shown in inset figure B as the "H" image of 1D surface PC in blue color. In our experiment, the character "H" can be seen in bluish violet color with viewing angle varying from 52° to 90°. Therefore, a multiplexing anti-counterfeiting film based on self-assemble photonic crystal (3D PC BPLC) and holography lithographic (1D/2D surface PC) photonic architectures has been fabricated on the BPLC encoded surface PCs, where different viewing angles carried different images. It is worth mentioned that, the colors of both images from BPLC and surface PCs are tunable by varying the lattice constant of BPLC and period of surface PCs, respectively. The designed structural color devices are stable and vivid, and would have potential applications in multiplexing display in information encryption and anti-counterfeiting.

III. Results and Discussion

Fig. 2(a) exhibits the polarized optical microscope (POM) image of the 3D PC BPLC film, which is aligned well by the rubbed PI treated substrate and shows vivid green color. The inserted picture is the Kossel diagram of the polymerized stabilized (PS) BPLC film which shows the symmetry of BPI [011] orientation. Figs. 2(b) and 3(c) show the scanning electron microscope (SEM) images of surface 1D PC and 2D PC encoded on the 3D PC BPLC film, respectively. The measured period of the 1D PC is 479 nm and the lattice constant of 2D PC is 482 nm, which both are consistent with the calculated 480 nm. Fig. 2(d) shows the multi-angle images when incident light source and detector are in the same direction which simulates the situation of scanning or shooting with cellphone and built-in flashlight. When the incident light is at the normal, the Bragg reflection of BPLC dominates (insert Fig. 1) which exhibits green color. The intrinsic viewing angles of BPLC are less than 30° [36], which is similar to our experiment results. As the detected angle is increasing, the diffraction of surface PC emerges (order "$m = 1$") from blue light to red light with angles of 30°, 35° and 40° (insert Figs. 2–4). Fig. 2(e) shows the reflective spectra of the PS-BPLC film (formed by M1) and solid BPLC film (formed by refilled M2) with the highest reflectivity of 44% and 45% at green color for normal incident, respectively. Comparing to PS-BPLC film consisted of liquid crystals and polymers, the solid BPLC film consists of all polymers bring to better thermo-stability while keeping similar reflection property. Therefore, the solid BPLC film is used in our experiment as the 3D PC BPLC film as well as the substrate for surface PC. The reflectivity at peak wavelength of solid BPLC film versus temperature from −50 °C to 260 °C is shown in Fig. 2(f). It can be seen that, the solid BPLC film is thermo-stable in range of −50∼260 °C. When the temperature is above 260 °C, the structure of solid BPLC film will be destroyed. Temperature below −50 °C is out of range of our measurement equipment, but the structure of solid BPLC film is intact and recoverable at −50 °C. In addition, the reflectance spectra from the surface 1D PC with diffractive angles of 30°, 35°, and 40° are shown in Fig. 2(g).

As shown in Fig. 3(a), the reflective angles of the gratings are determined by general diffraction condition [37]: $d(\sin\alpha + \sin\beta_m) = m\lambda$, where m is the diffraction order, which is an integer, d is the period of the grating (480 nm in our experiment), α is the incident angle, β_m is the diffraction angle at m order, λ is the wavelength of light. Fig. 3(a) demonstrates the schematic illustration of reflection in surface 1D PC. For a particular

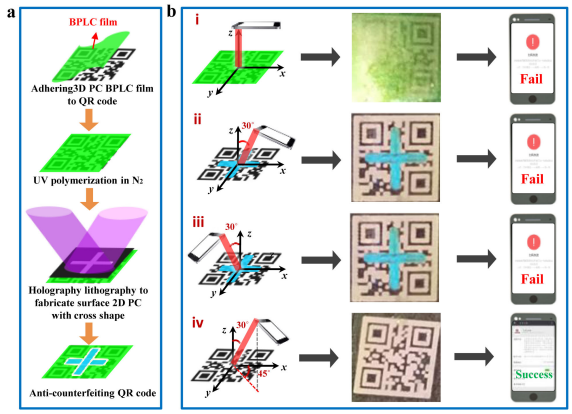

Fig. 4. (a) Fabrication process of the anti-counterfeiting QR code: the BPLC film (green) formed by the scaffold structures refilled with M2 is firstly adhered to the QR code (black). Then the sample is exposed under UV light for polymerization in N_2. After that, holography lithography is applied to fabricate the surface 2D PCs with shape of a cross. Finally an anti-counterfeiting QR code is fabricated. (b) Schematic illustration of anti-counterfeiting film in different scanning directions: (i) when the scanning direction of smartphone is along z axis, the 2D code is covered by the green color from the Bragg reflection of 3D BPLC film and the scanning result shows fail; (ii) when the scanning direction of smartphone has 30° angle with the z axis and in x-z plane, the QR code is covered with cross pattern in blue color and the scanning result shows fail; (iii) when the scanning direction of smartphone has 30° angle with the z axis in y-z plane, the QR code is covered with cross pattern in blue color and the scanning result shows fail; (iv) when the scanning direction of smartphone has 30° angle with the z axis and the projection of scanning direction in the x-y plane has 45° angle with the x axis, the QR code is covered by transparent film and the scanning result shows success.

wavelength, all values of m for which $|m\lambda/d| < 2$ correspond to physically realizable diffraction orders. The angles α, β_m are measured from the grating normal, the sign convention is positive if they are measured counter-clockwise. As the period of the grating is designed as 480 nm, the diffraction of $m = 1$ is in the same side of incident light, and the diffraction of $m = -1$ is beyond the limit which is forbidden.

In pure BPLC (Fig. 3(b)), the local refractive index variation leads to the Bragg reflection, and the reflection wavelength λ is determined by $\lambda = 2na/\sqrt{h^2 + k^2 + l^2}$, where n is the effective refractive index, a is the lattice constant, and h, k, l are the Miller indices [38]. In our experiment, the BPLC is aligned to BPI [011] orientation by the parallel alignment of PI on the substrate. Herein, the lattice constant a is about 240 nm, and the corresponding Bragg reflection wavelength is 536 nm in green color. The inset figures show the schematic structure of body-centered cubic crystal and the Kossel diagram of BPI. A strong selective Bragg reflection is preferred at the normal direction (as shown in Fig. 2(c)) in the pure BPLC when the incident light is normal to the plane.

Fig. 3(c) shows the schematic illustration of surface 2D PCs fabricated by two-step interference lithography that consists of two times two-beam interference. A squared matrix fabricated by two orthogonal gratings consists of two orthogonal periods and a diagonal period. The constant of the two orthogonal periods is equal to the interference period of 480 nm, and the constant of the diagonal period is $1/\sqrt{2}$ proportional to the interference period of 339 nm. The diffraction of surface 2D PCs is mainly composed of the three period structures. It is noticed that both 3D PC substrate and surface PCs are formed by BPLC.

Fig. 3(d) shows the reflective wavelength of multi-angle for diffraction order "$m = 1$" (visible region), where the incident angle α is equal to diffractive angle β_1 (order "$m = 1$") to simulate the situation of scanning by cellphone with built-in flashlight. For Grating 1 & 2, the diffractive wavelength varies from 406 nm to 679 nm while incident angle increases from 25° to 45°. In contrast, for Grating 3, the diffractive wavelength changes from 389 nm to 556 nm. It is because that the period of Grating 3 (339 nm) is much smaller than Grating 1 and Grating 2 (480 nm), leading to a larger viewing angle for the same wavelength. Base on this data in table, an anti-counterfeiting film can be designed in range of 25°∼30° incident and viewing angle, where a blue light will be observed from Grating 1&2 while a UV light will be observed from Grating 3. The image information is different when observing from directions along Grating 1 & 2 or Grating 3 even keeping the same incident angle α in 2D surface PC.

Fig. 4(a) depict the fabrication process of QR code with cryptographic functionality through our proposed multiplexing anti-counterfeiting film based on self-assemble 3D PC BPLC film and holography lithography 1D/2D surface PC architectures. The BPLC film (green) formed by the scaffold structures refilled with M2 is firstly adhered to the QR code (black). Then the sample is exposed under UV light for polymerization in N_2. After that, holography lithography is applied to fabricate the surface 2D PCs with shape of a cross. Finally, an anti-counterfeiting QR code is fabricated.

The schematic illustration of anti-counterfeiting film in different scanning directions is demonstrated in Fig. 4(b). The anti-counterfeiting QR code is scanned by the smartphone, the incident light source is offered by the built-in flashlight of smartphone. Scanning with angles less than 40° is the convenient scanning situations according to our custom with smartphone. To simulate these situations, the incident angle and diffractive angle are equal. In case i, when the scanning direction of smartphone is along z axis, the 2D code is covered by the green color from the 3D BPLC film where the Bragg reflection dominates and the scanning result shows fail. In this case, the reflection of BPLC protects the QR code in small viewing angles. In case ii, the viewing angle is increased. Since the reflective wavelength of 2D PCs varies from ultraviolet light to visible light; when the scanning direction of smartphone has 30° angle with the z axis and in x-z plane (along the direction of Grating 1), the diffraction of Grating1 dominates with blue light, the QR code is covered with cross pattern in blue color and the scanning result shows fail. In case iii, the viewing direction in 3D space is twisted. When the scanning direction of smartphone has 30° angle with the z axis in y-z plane (along the direction of Grating 2), similarly the diffraction of Grating 2 dominates with blue light, the QR code is also covered with a cross pattern in blue color and the scanning result shows fail. In case iv, the viewing direction in 3D space is twisted to the diagonal of x,y-axis. When the scanning direction of smartphone has 30° angle with the z axis and the projection of scanning direction in the x-y plane has 45° angle with the x axis (along the direction of Grating 3), the diffraction of Grating 3 dominates with UV light, the QR code is covered by transparent film in visible range and the scanning result is success. Among these four cases, scanning in three cases lead to fail output where the anti-counterfeiting QR code is under protection while scanning in the last case lead to success output where the anti-counterfeiting QR code is open access.

IV. Materials

M1: liquid crystal host HTG135200-100 ($n_e = 1.717$, $n_o = 1.513$ of 589 nm at 20 °C) 80.5 wt. %, chiral dopant R5011 (HTG $= 126\ \mu m^{-1}$) 3.5 wt. %, monomer RM257 10 wt. %, polymer TMPTA 5 wt. %, photo initiator 1173 1wt. %. M2: liquid crystal monomer HRM1001-002 99 wt. %, photo initiator 1173 1wt. % (all got from Hecheng Display). M3: photoresist mr-P 1202LIL (purchased from Micro Resist Technology).

V. Conclusion

In summary, we proposed an optical multiplexing anti-counterfeiting film based on self-assembled 3D PC BPLC encoded with holography lithographic 1D/2D surface PC. 1D/2D surface photonic crystal with different shape can be easily encoded by holography lithographic technology on the surface of 3D self-assembled photonic crystal BPLC to form a bilayer structure with multi-structural colors. The proposed bilayer structure can exhibit multi-images with different angles in 3D space, leading to multiple encryptions with information protection or access permission. Quick response (QR) code with cryptographic functionality through our proposed multiplexing anti-counterfeiting film based on bilayer structural color is also demonstrated with the smartphone. The proposed strategy for optical multiplexing anti-counterfeiting film is low-cost, easy-fabricated, time saving, stable and flexible, capable for promising perspective in information security level and storage density, and offering potential application in anti-counterfeiting.

References

[1] Z. Li *et al.*, "Photoresponsive supramolecular coordination polyelectrolyte as smart anticounterfeiting inks," *Nat. Commun.*, vol. 12, 2021, Art. no. 1363.

[2] Y. Liu *et al.*, "Unclonable perovskite fluorescent dots with fingerprint pattern for multilevel anticounterfeiting," *ACS Appl. Mater. Interfaces*, vol. 12, pp. 39649–39656, 2020.

[3] J. Liu *et al.*, "Simultaneously excited downshifting/upconversion luminescence from lanthanide-doped core/shell fluoride nanoparticles for multimode anticounterfeiting," *Adv. Funct. Mater.*, vol. 28, 2018, Art. no. 1707365.

[4] D. Li, L. Tang, J. Wang, X. Liu, and Y. Ying, "Multidimensional SERS barcodes on flexible patterned plasmonic metafilm for anticounterfeiting applications," *Adv. Opt. Mater.*, vol. 4, 2016, Art. no. 1475.

[5] I.-H. Lee *et al.*, "Selective photonic printing based on anisotropic Fabry-Perot resonators for dual-image holography and anti-counterfeiting," *Opt. Exp.*, vol. 27, pp. 24512–24523, 2019.

[6] Z. Li *et al.*, "Photoresponsive supramolecular coordination polyelectrolyte as smart anticounterfeiting inks," *Nat. Commun.*, vol. 12, 2021, Art. no. 1363.

[7] C. Fan *et al.*, "Fluorescent nitrogen-doped carbon dots via single-step synthesis applied as fluorescent probe for the detection of Fe^{3+} ions and anti-counterfeiting inks," *Nano*, vol. 13, 2018, Art. no. 1850097.

[8] K. T. P. Lim, H. Liu, Y. Liu, and J. K. W. Yang, "Holographic colour prints for enhanced optical security by combined phase and amplitude control," *Nat. Commun.*, vol. 10, 2019, Art. no. 25.

[9] X. Zhang *et al.*, "Holographic polymer nanocomposites with simultaneously boosted diffraction efficiency and upconversion photoluminescence," *Compos. Sci. Technol.*, vol. 181, 2019, Art. no. 107705.

[10] A. F. Smith and S. E. Skrabalak, "Metal nanomaterials for optical anticounterfeit labels," *J. Mater. Chem. C*, vol. 5, pp. 3207–3215, 2017.

[11] L. Qin *et al.*, "Geminate labels programmed by two-tone microdroplets combining structural and fluorescent color," *Nat. Commun.*, vol. 12, 2021, Art. no. 699.

[12] X. Lai *et al.*, "Bioinspired Quasi-3D multiplexed anti-counterfeit imaging via self-assembled and nanoimprinted photonic architectures," *Adv. Mater.*, vol. 34, 2022, Art. no. 2107243.

[13] A. Hazra, U. Mondal, S. Mandal, and P. Banerjee, "Advancement in functionalized luminescent frameworks and their prospective applications as inkjet-printed sensors and anti-counterfeit materials," *Dalton Trans.*, vol. 50, pp. 8657–8670, 2021.

[14] P. Kumar, S. Singh, and B. K. Gupta, "Future prospects of luminescent nanomaterial based security inks: From synthesis to anti-counterfeiting applications," *Nanoscale*, vol. 8, pp. 14297–14340, 2016.

[15] R. D. Hersch, P. Donzé, and S. Chosson, "Color images visible under UV light," *ACM Trans. Graph.*, vol. 26, 2007, Art. no. 75.

[16] Z. Xuan, J. Li, Q. Liu, F. Yi, S. Wang, and W. Lu, "Artificial structural colors and applications," *Innovation*, vol. 2, 2021, Art. no. 100081.

[17] Y. Gao, "On the use of overt anti-counterfeiting technologies," *Mark. Sci.*, vol. 37, pp. 403–424, 2018.

[18] E. Yablonovitch, T. J. Gmitter, and K. M. Leung, "Photonic band structure: The face-centered-cubic case employing nonspherical atoms," *Phys. Rev. Lett.*, vol. 67, pp. 2295–2298, 1991.

[19] Z. Gao, C. Huang, D. Yang, H. Zhang, J. Guo, and J. Wei, "Dual-mode multicolored photonic crystal patterns enabled by ultraviolet-responsive core-shell colloidal spheres," *Dyes Pigm.*, vol. 148, pp. 108–117, 2018.

[20] F. Meseguer, A. Blanco, H. Miguez, F. Garcia-Santamaria, M. Ibisate, and C. Lopez, "Synthesis of inverse opals," *Colloid. Surf. A*, vol. 202, pp. 281–290, 2002.

[21] Z. Gao, C. Huang, D. Yang, H. Zhang, J. Guo, and J. Wei, "Highly stretchable photonic crystal hydrogels for a sensitive mechanochromic sensor and direct ink writing," *Chem. Mater.*, vol. 31, pp. 8918–8926, 2019.

[22] H. Wang, Y. Liu, Z. Chen, L. Sun, and Y. Zhao, "Anisotropic structural color particles from colloidal phase separation," *Sci. Adv.*, vol. 6, 2020, Art. no. 1438.

[23] H. Stegemeyer, T. H. Blümel, K. Hiltrop, H. Onusseit, and F. Porsch, "Thermodynamic, structural and morphological studies on liquid-crystalline blue phases," *Liq. Cryst.*, vol. 1, pp. 3–28, 1986.

[24] M. E. McConney, M. Rumi, N. P. Godman, U. N. Tohgha, and T. J. Bunning, "Photoresponsive structural color in liquid crystalline materials," *Adv. Opt. Mater.*, vol. 7, 2019, Art. no. 1900429.

[25] H. Kikuchi, M. Yokota, Y. Hisakado, H. Yang, and T. Kajiyama, "Polymer-stabilized liquid crystal blue phases," *Nat. Mater.*, vol. 1, pp. 64–68, 2002.

[26] G. Nordendorf, A. Hoischen, J. Schmidtke, D. Wilkes, and H.-S. Kitzerow, "Polymer-stabilized blue phases: Promising mesophases for a new generation of liquid crystal displays," *Polym. Adv. Technol.*, vol. 25, pp. 1195–1207, 2014.

[27] F. Castles *et al.*, "Blue-phase templated fabrication of three-dimensional nanostructures for photonic applications," *Nat. Mater.*, vol. 11, pp. 599–603, 2012.

[28] F. Castles *et al.*, "Stretchable liquid-crystal blue-phase gels," *Nat. Mater.*, vol. 13, pp. 817–821, 2014.

[29] M. Wang *et al.*, "Asymmetric tunable photonic bandgaps in self-organized 3D nanostructure of polymer-stabilized blue phase I modulated by voltage polarity," *Adv. Funct. Mater.*, vol. 27, 2017, Art. no. 1702261.

[30] M. Wang *et al.*, "Bias-polarity dependent bidirectional modulation of photonic bandgap in a nanoengineered 3D blue phase polymer scaffold for tunable laser application," *Adv. Opt. Mater.*, vol. 6, 2018, Art. no. 1800409.

[31] J. Yang *et al.*, "Printable photonic polymer coating based on a monodomain blue phase liquid crystal network," *J. Mater. Chem. C*, vol. 7, pp. 13764–13769, 2019.

[32] J. Yang *et al.*, "Photonic shape memory polymer based on liquid crystalline blue phase films," *ACS Appl. Mater. Interfaces*, vol. 11, pp. 46124–46131, 2019.

[33] Y.-S. Zhang, S.-A. Jiang, J.-D. Lin, P.-C. Yang, and C.-R. Lee, "Stretchable freestanding films of 3D nanocrystalline blue phase elastomer and their tunable applications," *Adv. Opt. Mater.*, vol. 9, 2021, Art. no. 2001427.

[34] X. Xu *et al.*, "Electrically switchable, hyper-reflective blue phase liquid crystals films," *Adv. Opt. Mater.*, vol. 6, 2018, Art. no. 1700891.

[35] X. Xu, Y. Liu, and D. Luo, "Flexible blue phase liquid crystal film with high stability based on polymerized liquid crystals," *Liq. Cryst.*, vol. 47, pp. 399–403, 2020.

[36] J. Yan, S.-T. Wu, K.-L. Cheng, and J.-W. Shiu, "A full-color reflective display using polymer-stabilized blue phase liquid crystal," *Appl. Phys. Lett.*, vol. 102, 2013, Art. no. 081102.

[37] C. Palmer, *Diffraction Grating Handbook*. Rochester, NY, USA: Richardson Gratings Lab., 2000, ch. 2, pp. 19–21.

[38] H. Kikuchi, "Liquid crystalline blue phases," *Struct. Bond*, vol. 128, pp. 99–117, 2008.